Empirical Dry-Friction Modeling in a Forced Oscillator Using Chaos

B. F. Feeny
Associate Professor
Department of Mechanical Engineering
Michigan State University
East Lansing, MI 48824

F. C. Moon
Professor
Sibley School of Mechanical Engineering
Cornell University
Ithaca, NY 14853

ABSTRACT

The coefficient of friction is measured during relative oscillation between sliding surfaces. Measurements are made during regular oscillations in which the excitation has a modulated amplitude, and during chaotic oscillations in which the excitation amplitude is fixed. The friction force is measured for paper on paper, and titanium on titanium. A friction law is derived based on observations from the measurements. This friction law is applied to a simulation model of an experimental forced oscillator. The simulated and experimental oscillators have similar qualitative dynamical features in the phase space.

1 INTRODUCTION

Choosing a proper friction law for modeling a vibrating system is a nontrivial task. Friction is dynamical, exhibiting some phenomena strictly associated with the contact interface, and others involving interactions between the contact and the structure (Tworzydlo *et al.* 1994). Friction models range from the simple Coulomb law to complicated surface/tribological descriptions. For an idea of the span of these models, we refer the reader to review articles by Oden and Martins (1986), Ibrahim (1994a, 1994b), and Armstrong-Helouvry *et al.* (1994). The degree to which the friction model incorporates friction phenomena determines how well the dynamics of the entire structure are represented, which in turn effects analyses, prediction, and control. As stated by Armstrong-Helouvry *et al.* (1994), "A successful design and analysis of friction compensators depends heavily upon the quality of the friction model." This idea applies to dynamical systems in general, such as in manufacturing processes, earthquake studies, and frictional noise generation.

Models are typically chosen to accommodate the particular phenomenon exhibited by the system at hand (Ibrahim, 1994a). The Coulomb friction law, together with static friction, are sufficient for modeling stick-slip in forced lumped oscillators (Den Hartog, 1931; Shaw, 1986). A friction law of the form $F = f(v)$,where v is velocity and $f'(v)$ can be negative, is sufficient to explain self-excited oscillations (Brockley and Ko, 1970). But it does not describe the hysteresis in the (f,v)-plane, as has been observed in sliding rocks (Rice and Ruina, 1983). Other models describe hysteresis (Rice and Ruina, 1983; Ruina, 1985), but are not applicable for relative motion which changes direction. (Ruina (1988) has suggested a modification to accommodate direction changes.) Oden and Martins (1985) and Dankowicz (1999) formulated friction models

which include the effects of normal vibrations. Friction hysteresis has been modeled by bristle models (Haessig and Friedland, 1991) and contact compliance (Liang and Feeny, 1998a).

To assist in modeling, many researchers have measured friction. The work of Bowden and Tabor (e.g. 1967) consists of the measurement of various friction properties for many materials. Hunt *et al.* (1965) and Antoniou *et al.* (1976) estimated friction by applying Lienard's construction to measurements of displacement in a uniform direction. Using a load cell, Aylward and Karis (1985) measured the frictional force between polymers sliding in a uniform direction. Similar measurements by Rorrer *et al.* (1992) emphasized stick-slip transitions. Dieterich and Conrad (1984) measured hysteresis in sliding rocks during changes in relative velocity under various conditions of humidity. Rice and Ruina (1983) measured hysteresis in the sliding friction of rocks using a torsional load cell. Oden and Martins (1985) have made measurements which support their model, in which system effectively takes a constant coefficient of friction, but a varying effective normal load. Polycarpou and Soom (1992) measured lubricated friction during unidirectional stick-slip and observed frictional delay.

There are also examples of work on friction in oscillators with direction reversals. Marui and Kato (1986) experimentally studied stick-slip in a forced oscillator, and included friction measurements. Srinivasan (1988) measured equivalent friction coefficients for tungsten-coated titanium surfaces whose relative displacement was sinusoidal, for various frequencies, amplitudes, and normal loads. Wojewoda *et al.* (1992) measured friction during oscillations which reversed direction, and suggested that the friction force itself might be chaotic. Among many other examples of friction measurements during oscillations are Hinrichs et al. (1998), Liang and Feeny (1998a, 1998b), Ibrahim (2000), and Filippi et al. (2004).

Many more examples of friction measurements and friction induced dynamics can be found in the aforementioned review articles.

The goal of this work is to model the friction in a forced, chaotic mechanical oscillator. Rather than pursuing developments in the knowledge of the friction mechanism itself, we seek a friction law which can be implemented in the differential equations of motion. Toward our goal, we measure the friction force versus displacement and velocity, and display the friction characteristic in surface plots, as has been done in characterizing pin joints (Crawley and Aubert, 1986; Ikegami *et al.,* 1986; Chapman *et al.,* 1987). We use an amplitude-modulated input to sweep the response through an area in phase space. Since the motivational oscillator is chaotic, and chaotic systems tend to sweep the phase space, we then make friction measurements during chaos, and consider the relationship between chaos histories and dynamical friction characteristics. We infer a friction model from measurements. The resulting friction law qualitatively models the dynamics of the experimental oscillator with some improvement over the commonly used Coulomb law.

2 MOTIVATIONAL EXPERIMENTAL OSCILLATOR

Leonardo da Vinci (1452-1519) and Amontons in 1699 (referenced through Bowden and Tabor, 1967) noticed that the force of sliding friction is roughly proportional to the normal load at the contact surface. Our motivational oscillator exploits this idea.

The oscillator consisted of a mass attached to the end of a cantilevered elastic beam. The mass had titanium plates on both sides, providing surfaces for sliding friction. Spring-loaded titanium pads rested against the titanium plates. We used titanium because it is relatively light and tough, and therefore a candidate for flight and space applications (Srinivasan, 1988). The experimental set-up and mechanics model (top view) are shown in Figure 1. Unlike the figure, the titanium plates were not parallel in the direction of sliding, and thus a displacement of the mass caused a change in the force on the spring-loaded pads. Hence a change in displacement caused a change in normal load and frictional force.

The elastic beam, mass and pressure pads were fixed to a common frame which was excited harmonically by an electromagnetic shaker. In place of the beam with semiconductor strain gages in Figure 1 was a rigid attachment. Strain gages attached to the elastic beam were used to sense the displacement of the mass relative to the oscillating frame. An analog differentiator was used to obtain the velocity of the mass. The behavior of the differentiator was "ideal" for frequencies up to 150 Hz. The beam and mass had a fundamental natural frequency of 2.4 Hz with the friction removed. The frequency of the second mode was 37 Hz. The excitation frequency was typically in the range of 2.5 Hz to 6 Hz, with an amplitude typically in the range of 8-12 mm. The first-mode damping ratio was $\zeta \approx 0.015$.

The oscillator exhibits periodic and chaotic behaviors, depending on parameter values. An example of a chaotic response to a periodic excitation at 4.2 Hz is shown in a three-dimensional phase space projected into the two dimensions of Figure 2. In cylindrical coordinates, the figure displays the displacement as the radial axis, time (modulo the driving period) as the circumferential axis, and velocity as the longitudinal axis. The trajectory flows clockwise. During a single driving period, segments of the trajectory which lie on the inside of the flattened toroidal structure flow with a negative velocity, then with a positive velocity, and as they return near the outside of the toroidal structure, they overshoot the zero-velocity plane. Segments of the trajectory which lie on the outside of the toroidal sheet flow with a negative velocity, and then stick until they return again near the outside of the toroidal structure. The latter orbits spend a longer amount of time being stuck than others. This is important because the friction measurements turn out to have different characteristics in heavily sticking motion than in lightly sticking motion, and we would like to identify these characteristics on the friction plots with features in the phase portraits.

Further details regarding the experimental setup and dynamical response can be found in Feeny and Moon (1994).

In modeling this oscillator, we need an appropriate friction law. A satisfying qualitative model would predict the toroidal structure. A detail to be modeled would be the overshoot of the zero-velocity plane.

3 EXPERIMENTAL METHOD FOR FRICTION MEASUREMENT

3.1 Experimental Apparatus

The experimental set-up was similar to that of the motivational oscillator in Section 2, and is shown in Figure 1. For some measurements, the titanium surfaces were coated with paper. Paper was studied for its importance to printer technology, and also to observe the coupled structural-frictional behavior under another set of circumstances.

For the regular oscillator, the plates were nearly parallel, so that the normal load should be nearly constant We used two chaotic oscillators. For the first chaotic oscillator, the plates were not parallel in the direction of sliding, as in Section 2. For the second chaotic oscillator, the plates were parallel, but magnets were mounted to the frame to provide two wells in the stiffness potential. The two- well oscillator (in particular the Duffing oscillator) has been studied thoroughly as an example which exhibits many characteristics of nonlinear behavior (Nayfeh and Mook, 1979; Guckenheimer and Holmes, 1983; Moon, 1992), including chaos. The effect of dry friction on such oscillators has been examined by Awrejcewicz (1986) and Narayanan and Jayaraman (1991).

The dimensions of the components discussed above are listed in Table 1. Beam I, Beam II, Beam III, and Beam IV refer respectively to the beams with paper-coated parallel plates, titanium parallel plates, skewed plates, and a two-well stiffness potential. Each beam was made of stainless steel. Beam I with the attached mass had a fundamental frequency of 3.6 Hz, while

the other beams each had a fundamental frequency of 2.4 Hz. Beam II, for example, had a second modal frequency of 37 Hz.

The excitation and sensing methods for the mass-beam dynamics were the same as in Section 2. The excitation was applied at frequencies ranging from 2.5 Hz to 5.0 Hz, and at amplitudes ranging from 0-12 mm.

Semiconductor strain gages on a stainless steel beam connecting the pressure pads to the frame formed a load cell for sensing the transverse frictional force. The members which transmitted the frictional load to this frictional load cell were brass feeler gages 0.5 inches wide and 0.006 inches thick. The normal loads were applied by cantilevered elastic (stainless steel) beams. Strain gages on these beams were used to sense the normal load. Normal loads in the range of 0.1 N to 0.5 N were used during these experiments. Teflon and 3M anti-stick paper (for poster stickers) made the contact between the normal load apparatus and the pressure pads. Dimensions of the beams that comprise the frictional load cell and the normal load cell are listed in Table 1.

In all experiments, the displacement was measured using a strain gage signal from the elastic beam. This signal passed through an ITHACO 4213 Electronic Filter with a cutoff frequency of 25 Hz, and then through an analog differentiator. The frictional force signal came from the load cell, and the input was measured with a linear variable differential transducer, and sent through an analog filter with a cutoff frequency of 25 Hz. All signals--displacement, velocity, frictional force, normal load, and input--were sent to a multi- channeled data-acquisition computer system (MASSCOMP), which converted them to digital signals. All signals then passed through a digital filter set at 25 Hz cutoff. Experimental oscillations displayed in this paper were driven in the range of 2.5-5.0 Hz.

3.2 Materials and Preparation

The paper used was Xerox 3R729, substance 20, 75 g/m2, white, and long grain. The paper was fastened to titanium plates and pads using 3M Spray Mount Artist's Adhesive, catalog no. 6065. It is described as "low soak-in", The mount was made by lightly spraying the back of the paper, and sticking it to the titanium plates. After mounting, a light brushing with acetone was applied to the contact surfaces,

For titanium versus titanium, the pads and plates were wiped with acetone, and then some sliding took place prior to measurements. Beyond cleaning, the surface of the titanium was not prepared. It was in a partially worn state from previous dynamics experiments. This may not be conducive to tribological understanding of surface interfaces, but it is reasonable for the low-order modeling of a system which is operating in a worn state, as is the case of our motivational oscillator. Care was taken to not handle any friction surfaces, since finger oils would alter friction properties.

The experiment was conducted near 74° F and 47% relative humidity.

3.3 Friction Measurements

The measurements must account for the load-cell dynamics. The friction apparatus, which includes the friction pads and load cell, is an inertially excited dynamic system (see Figure 1 (b)). For general discussions on the dynamics of transducers under frictional excitation, see Streator and Bogy (1992) or Streator(1992). Assuming that the oscillator and load cell are linear, harmonically driven, and have one degree of freedom, the governing equations of motion are

$$m\ddot{x} + c\dot{x} + kx + f = m\Omega^2 a\cos(\Omega t),$$

$$m_l\ddot{y} + c_l\dot{y} + k_l y - f = m_l\Omega^2 a\cos(\Omega t),$$

where x is the deflection of the oscillator mass, y is the deflection of the load cell, a is the amplitude of the excited frame, and f is the friction force between the pads and plates. The subscript l indicates load-cell parameters, $c\dot{x}$ and $c_l\dot{y}$ are linear representations of small material and viscous damping that may be present. The fundamental frequency of the load cell was measured as 19.3 Hz, with a damping ratio $\zeta_l \approx 0.016$.

The effective mass of the load cell can be estimated by its total mass m_l = 12.6 g. The stiffness of the load cell can be estimated using the dimensions of the load-cell beam, and the elastic modulus of steel, to obtain k_l = 3.48 x 10^5 g/s^2. If the motion of the load cell were sinusoidal, we would have $y = b\cos(\Omega t - \phi)$, $\dot{y} = -b\Omega\sin(\Omega t - \phi)$, and $\ddot{y} = b\Omega^2\cos(\Omega t - \phi)$. Comparing the magnitudes of the load-cell restoring force $k_l y$ with the viscous damping force $c_l\dot{y}$ yields $|c_l\dot{y}|/|k_l y| = 2.9c_l\Omega\times10^{-6}$, which is small for reasonable values of c_l and for values of Ω in which we are interested. Comparing the magnitudes of the load-cell restoring force $k_l y$ with the inertial force $m_l\ddot{y}$ yields $|m_l\ddot{y}|/|k_l y| = 3.6\Omega^2\times10^{-5}$, which is small (in the range of 0.009-0.035) for values of Ω in which we are interested. The compliance in the friction contact can lead to hysteresis during sliding reversals and friction oscillations during stick-slip (Liang and Feeny, 1998a).

The deflection of the load cell is proportional to its strain. Therefore $k_l y$ is proportional to the load-cell signal S through some constant α, i.e. $k_l y = \alpha S$. Thus, neglecting the dynamical effects, the frictional force can be approximated as

$$f = \alpha S - m_l\Omega^2 a\cos(\Omega t). \qquad (1)$$

During a measurement in a regular oscillator, the input is amplitude modulated (by hand) so that the motion sweeps a region in phase space. The amplitude varies in the range of 0 to 12 mm.

The chaotic oscillators tend to sweep the phase space with a fixed input amplitude. During the motion of a mass with non-parallel plates, the spring-loaded normal load will increase as the wedge in the plates displaces the friction pads.

3.4 Computations

A computer program read and calibrated 800 samples of displacement, velocity, friction force, normal load, and input signals (the frictional-force signal was the sum of two frictional loads in the oscillator, and the normal-load signal represented the sum of two nor-mal loads in the oscillator). It then removed the approximate DC drift in the friction force and input signals. It used equation (1) to approximate the friction force on the oscillator, and divided by the instantaneous normal load to yield the coefficient of friction. These 800 values of coefficient of friction, displacement, and velocity, were used to create surface plots from the data.

4 SOURCES OF EXPERIMENTAL ERROR

The measurements relate the coefficient of friction versus displacement and velocity. The displacement and frictional force were sensed by strain gages in beams. The presence of higher modes of deformation in these beams may have some effect on interpreting displacements and forces. However, the difference in the first and second modal frequencies was enough that we

expect the contribution of higher modes to be small. Also, rotational components in frictional sliding could influence the frictional strain signal.

Since both the friction pads and the beam were attached a cantilevered beams, there will be some relative rotation between them when they deform. This could interfere with the possibility of achieving stick-slip. However, stick-slip was clearly observed, comparable to the case in which the load-cell beam is replaced by a rigid member. Thus, this rotational effect on stick-slip is taken to be minor.

The frictional load cell could undergo elastic deformation, whereas the motivational oscillator had a rigid friction attachment. The amount of deflection in the contact pads is estimated in section 5.1.

The strain gage readings in each normal-load cell (on each side of the load cell) were calibrated to convert volts to grams, i.e. $N_1 = c_1 v_1$ and $N_2 = c_2 v_2$, where v_1 and v_2 represent voltage readings from each normal-load cell. The total normal load was $N = N_1 + N_2$. (Recall from Section 3.4 that we divide the sum of two frictional loads by the sum of two normal loads.) However, the normal load strain gages were all in the same wheatstone bridge. Therefore, on a readout, we only saw $V = v_1 + v_2$. Fortunately, $c_1 \approx c_2$, and we lose little by assuming them equal in the computations.

The pressure pads were mounted to flimsy cantilevered beams, which were designed to transmit the transverse frictional load to the friction load cell. The normal load was applied to the pressure pads via these cantilevered beams. Thus, the deformation of the cantilevered beams supporting the pressure pads absorbed some of the measured normal load. On the other hand, there was typically some degree of incidental contact between the pressure pads and the friction plates prior to application of the normal loads. The upshot is that there is some deviation between the actual normal load and the measured normal load due to the experimental set up. This deviation would affect the calculation of the coefficient of friction, $\mu = f/N$. We expect the accuracy to increase as the normal load increases. In Figure 3 the normal load is plotted verses the displacement for experiments on oscillations with "parallel" plates as well as oscillations with skewed plates. For the case of skewed plates, there is a nearly linear variation in normal load, as expected for planar plates, for a large range of normal loads. The "parallel" plates also show some variation in the normal load with displacement.

The application of the normal load to the back of the pressure pad introduces a dry contact in the friction apparatus, located at point A in the diagram of Figure 1. These contact materials are and nonstick paper (used by 3M to package poster stickers). The contact is noticeably more slippery than teflon on teflon, which has a coefficient of friction between 0.04 and 0.1 (Bowden and Tabor, 1967). According to our estimation, the static coefficient of friction between these surfaces, for moderate loading, is between 0.03 and 0.05. Thus, the contribution of this contact in the friction measurement should be negligible.

Filtering distorts components of the friction history associated with high frequencies, such as a spike due to the static friction, a nearly discontinuous switch from positive to negative friction (as in Coulomb friction), and normal-surface vibrations. Tribologists usually prefer to see these high-frequency components of the measurement. For our application, a low-frequency oscillator behaves as a low-pass filter, and thus high-frequency components of a friction model will not affect its low-order dynamics. We compared the friction plots for the skewed-plates oscillator with cutoff frequencies (in the MASSCOMP) of 25 Hz and 100 Hz, and saw no obvious difference.

5 RESULTS

5.1 Friction Measurements In the Regular Oscillator

First we present results on the regular oscillator with parallel plates. Measurements for paper on paper are displayed in Figures 4. As an experimental phase trajectory goes from negative to positive velocity, the friction measurement abruptly leaves the negative value (which we might call $-\mu_s$.), and gradually reaches the positive value (μ_k). Similarly, as a trajectory goes from positive to negative velocity, the force measurement abruptly leaves the positive value, and gradually reaches the negative value. This yields a hysteresis loop in the friction-velocity plane. For large motion, the hysteresis loop seems more pronounced than for small motion.

The features of the friction measurements for titanium on titanium are similar to those for paper on paper (Figure 5).

Paper has a higher coefficient of friction than titanium. The measured coefficient of sliding friction of paper on paper (at normal loads ranging from 0.12 N to 0.17 N) ranges from 0.6 to 1.0, while that of titanium on titanium (at normal loads ranging from 0.10 N to 0.16 N) ranges from as low as 0.2 to 0.5.

Based on this range of normal loads and friction coefficients, along with the load-cell stiffness and the beam attachments, the contact point may have deflected with amplitudes as high as 2.5 mm in the highest-loading case, and as low as 0.24 mm in the lowest-loading case. This conservative estimate accounts for the amplification of the load-cell rotation by the attachment beams. In Figure 4(c), however, little deformation is detected during a loaded stick.

5.2 Friction Measurements from Chaotic Oscillators

Measurements for the oscillator with skewed plates are shown in Figures 6 and 7. The qualitative features of friction observed in the regular oscillators are apparent in the measurements from the oscillator with skewed plates. In the region where motion is small and sticking and the normal load is large, the change in friction with respect to velocity is steeper than where the friction is light.

Friction measurements for paper on paper were also made using the two-well oscillator with applied friction, as shown in Figures 8. Features of the friction are more difficult to distinguish since the character of its chaos is slightly more complex than that of the oscillator with skewed plates. Steep spiky features are intermixed with smoother features. However, for large displacements, where the chaos has a more consistent character, and motion is nonsticking, the frictional characteristic is smoother and more hysteretic, which is consistent with observations from the regular oscillator.

6 INTERPRETATION AND DISCUSSION

The forced data can be interpreted as following some kind of Coulomb-like backbone in the friction relation, about which there is some variation. This variation could be due to frictional memory, or else experimental uncertainty such as load-cell dynamics, higher modes of the oscillator, relative rotation at the contact, or filtering. Frictional memory would compliment observations of Dieterich and Conrad (1984) and Rice and Ruina (1983). Possible interpretations raised are that the associated hidden state variable represents some effective contact time, or quantifies quality of contact. Klepp (1990) has suggested that relative acceleration may have some effect on friction. Indeed, it may be due to interactions between the contact dynamics and the elasticity of the beam. Other mechanisms may be at work. For example, friction oscillations

have been attributed to load cell dynamics in the past (Marui and Kato, 1986; Polycarpou and Soom, 1992; Liang and Feeny, 1998a).

A simple model for what we observe in this data would describe friction as a state which asymptotically approaches a Coulomb backbone function. An example of such a model could be expressed as

$$\ddot{x} + x + \theta = a(t), \tag{3}$$

$$\dot{\theta} = -\gamma(\theta - f(\dot{x})), \tag{4}$$

where $f(\dot{x})$ is the Coulomb backbone. The Coulomb backbone may be discontinuous, but the variable θ will be continuous in time. The friction θ in equations (3) and (4) has no explicit dependence on velocity, which is necessary to model certain friction phenomena in other systems (Rice and Ruina, 1983; Ruina, 1983). As $\gamma \to \infty$, this system (singularly perturbed) approaches the Coulomb oscillator.

A plot of the frictional force θ during a simulation of equations (3) and (4), with $a(t) = 2\cos(1.5t)\cos(1.5t/40)$, $f(\dot{x}) = \tanh(50\dot{x})$, and $\gamma = 10$, is shown in Figure 9. There is a strong resemblance with the experimental plots in Figures 4(a) and 5(a), although the asymptotic approach to the backbone function is at a slightly different rate.

Close examination of the friction-velocity plots reveals an unexpected feature. Measurements near zero velocity imply that, for a short interval of time, the mass experiences negative friction. This could be either a result of beam effects, load cell deflections, or an effect of unseen state variable in the friction. The friction model of equation (4) produces this feature. For the case of contact compliance or load-cell deflections, the hysteresis does not truly indicate negative friction, rather a brief negative force due to the loaded spring in the contact or load cell (Liang and Feeny, 1998a).

Our measurements in Figure 6 exhibit a dependence of the coefficient of friction on normal load (previous comments on normal load errors heeded). Static measurements also indicate some variation with respect to normal load (Feeny, 1990). In addition, the work of Linker and Dieterich (1992) and Bowden and Tabor (1967) suggests that the normal load affects friction characteristics.

If indeed friction is dependent on the motion *and* on one or more additional state variables, then this will come into play when deriving friction phenomena from the chaotic oscillators. The phase space in chaotic systems undergoes stretching and folding (Moon, 1992). Thus, neighboring orbits may have completely different recent histories. For example, it is conceivable that one trajectory is barely sticking, and a trajectory very nearby in the phase space is heavily sticking. In such case, neighboring points on a friction-force plot may contain significantly different information, causing the force plot to be rough, or to contain an average of different friction characteristics. (Augmenting the phase space with the hidden states may send these orbits far away from each other.) In the oscillator with skewed plates, there are regions of the phase space where motion is heavily sticking (due to higher friction loads) and regions where motion is lightly sticking. A nice aspect of this system is that it contains information about friction in heavily sticking oscillation, and information about friction in lightly sticking oscillation. It also includes information about friction under both high and low normal loads. With a little understanding about the nature of the chaotic dynamics of this system, we can extract the different types of information from one plot. The measurements of friction in the regular oscillator require several measurements under various conditions to obtain such information. However, it is easier to distinguish these varying conditions in the regular oscillator.

7 MODELING THE MOTIVATIONAL OSCILLATOR

We model the motivational oscillator with the nondimensional equations

$$\ddot{x} + 2\zeta\dot{x} + x + n(x)\theta = a\cos(\Omega t), \tag{5}$$

$$\dot{\theta} = -\gamma(\theta - \tanh(50\dot{x})), \tag{6}$$

The first three terms in equation (5) represent a linear mass-spring-dashpot. The varying normal load for a unilateral contact is modeled by $n(x) = 1 + kx, x > -1/k$,and $n(x) = 0, x < -1/k$. Thus the normal load varies linearly with displacement except when contact is lost, for which the normal load is zero. (A similar system with a bilateral contact has been studied by Anderson and Ferri, 1990). For illustration, we use two friction models. First, we model the system with equation (5) only, and with the Coulomb friction model, such that $\theta = sign(\dot{x}), \dot{x} \neq 0$, and $-1 \leq \theta \leq 1, \dot{x} = 0$. The geometry of this system's dynamics has been analyzed (Feeny, 1992). Second, the system is modeled with both equations (5) and (6), and the friction is modeled with the state variable 9 as in the previous section.

Numerical simulations of these systems reveal periodic and chaotic responses. For the parameters $k = 1.5$, $a = 1.9$, $\Omega = 1.25$, $\zeta = 0$ and $\gamma = 10$, the chaotic response is shown in Figure 10. The displacement is the radial axis, time $t(\text{mod } 2\pi/\Omega)$ is the circumferential axis, and velocity is the longitudinal axis. The Coulomb model alone produces a response which exhibits the stretching and folding toroidal branched manifold. Similar effects are obtained with smoothened versions of the Coulomb model (Feeny and Moon, 1989; 1994). However, the state-variable model leads to a response which exhibits the toroidal structure and the overshoot of the zero-velocity plane.

8 CONCLUSION

We have measured the dynamical coefficient of friction for paper on paper and titanium on titanium during oscillations which featured direction reversals. Measurements were made during regular and chaotic oscillations. The complexity of chaos can lead to complexity in the representation of the friction characteristic. We have derived a state-variable friction law based on the friction measurement observations. The state variable may represent pure frictional phenomena or friction-structure interaction.

The empirical friction model was applied to a motivational oscillator. The state-variable model produced the general features of the motivational oscillator, with some qualitative improvement over the Coulomb friction law.

The qualitative force characteristics are the same for titanium on titanium and paper on paper. This suggests that the low-order qualitative model for this structural system is not particularly material specific, and that the motivational oscillator would have similar qualitative low-order dynamical features under both situations.

It is desirable that some physical understanding complement the friction model (Armstrong-Helouvry *et al.* 1994; Ibrahim, 1994b). The target of future work will be to investigate the

possible role of phenomena such as rising static friction, normal surface vibration, coupling of the contact dynamics with the elastic structure, friction memory and delay, and acceleration, in the model. Such physical understanding is important in the design stage when considering the effect of parameters, for example on friction-induced vibration.

ACKNOWLEDGEMENTS

We thank Professor Andy Ruina for suggesting that we measure the frictional force in our oscillator, and for discussing state-variable friction laws. We also appreciate the comments of Professor Philip Holmes, the laboratory assistance of Bill Holmes, and the graphics work of Bill Feeny and Theresa Howley. This work was supported by grants from IBM, the ARO, and the AFOSR.

REFERENCES

Anderson. J. R., and Ferri, A. A., 1990, "Behavior of a single-degree-of-freedom system with a generalized friction law," *Journal of Sound and Vibration* **140**(2), pp. 287-304.

Antoniou, S. *S.,* Cameron, A., and Gentle, C. R., 1976, "The friction-speed relation from stick-slip data," *Wear* **36**, pp. 235- 254.

Armstrong-Helouvry, B., Dupont, P. and Canudas de Wit, *C.,* 1994, "A survey of models, analysis tools and compensation methods for the control of machines with friction." *Automatica* 30 (7), pp. 1083-1138.

Awrejcewicz, J., 1986, "Chaos in simple mechanical systems with friction." *Journal of Sound and Vibration* 109, pp. 178-180.

Aylward, L., and Karis, T., 1985, "Sliding friction between some commercial polymers under low load and velocity conditions in the limit of zero wear," *IBM Research Report,* RJ 4619 (49317).

Bowden, F. P., and Tabor, D., 1950, *Friction and Lubrication of Solids,* Clarendon Press, Oxford.

Bowden, F. P., and Tabor, D., 1967, *Friction and Lubrication,* Methuen and Co. Ltd., London.

Brockley, C. A. and Ko, P. L., 1970, "Quasi-harmonic friction- induced vibration," *Journal of Lubrication Technology* 92, pp. 550- 556.

Chapman, J. M., Shaw, F. H., and Russell. W. C., 1987, "Non- linear transient analysis of joint dominated structures," *AIAA Paper 87-0892,* pp. 568-577.

Crawley, E.F., and Aubert, A. C., 1986, "Identification of non- linear structural elements by force-state mapping," presented at the *Workshop on Structural Dynamics and Control Interaction of Flexible Structures,* Marshall Space Flight Center, Huntsville, Alabama, Apri122-24.

Dankowicz, H., 1999, "On the Modeling of Dynamic Friction Phenomena," *Zeitschrift fuer angewandte Mathematik und Mechanik* 79(6) pp. 399-409.

Den Hartog, J. P., 1931, "Forced vibrations with combined Coulomb and viscous friction," *Transactions of the ASME* 53, pp. 107-115.

Dieterich, J. H., and Conrad, G., 1984, "Effect of humidity on time- and velocity-dependent friction in rocks," *Journal of Geophysical Research,* 89(B6), pp. 4196-4202.

Feeny, B. F., 1990, *Chaos and Friction,* doctoral thesis, Cornell University.

Feeny, B., 1992, "A nonsmooth Coulomb friction oscillator," *Physica D* 59, pp. 25-38.

Feeny, B. F., and Moon, F. C., 1989, "Autocorrelation on symbol dynamics for a chaotic dry-friction oscillator," *Physics Letters A* **141** (8,9) 397-400.

Feeny, B. F., and Moon, F. C., 1994 "Chaos in a forced dry-friction oscillator: experiment and numerical modeling," *Journal of Sound and Vibration* 170, pp. 303-323.

Filippi S., Akay A., May A., Gola MM., 2004 "Measurement of tangential contact hysteresis during microslip," *Journal of Tribology-Transactions of the ASME* 126 (3), pp. 482-489.

Guckenheimer, J., and Holmes, P. J., 1983, *Nonlinear Oscillations, Dynamical Systems, and Bifurcations of Vector Fields,* Springer-Verlag, New York.

Haessig, D.A. and Friedland, B., 1991, "On the modeling and simulation of friction," *Journal of Dynamic Systems, Measurement and Control*, Vol.113, pp. 354-362.

Hinrichs, N., Osetreich, M., and Popp, K., 1998, "On the modeling of friction oscillator," *Journal of Sound and Vibration*, 216(3), pp. 435-459.

Hunt, J.B., Torbe, I.. and Spencer, G. C., 1965, "The phase-plane analysis of sliding motion," *Wear,* Vol. 8, pp. 455-465.

Ibrahim, R. A., 1994a, "Friction-induced vibration, chatter, squeal, and chaos: part I-mechanics of contact and friction," *Applied Mechanics Reviews* 47(7), pp. 209-226.

Ibrahim, R. A., 1994b, "Friction-induced vibration, chatter, squeal, and chaos: part II-dynamics and modeling," *Applied Mechanics Reviews* 47(7), pp. 227-255.

Ibrahim, R.A., Madhavan S., Qiao, S.L., Chang, W.K, 2000, "Experimental investigation of friction-induced noise in disc brake systems," *International Journal of Vehicle Design*, 23 (3-4), pp. 218-240.

Ikegami, R., Church, S. M., Keinhloz, D. A., and Fowler, B. L., 1986, "Experimental characterization of deployable trusses and joints," presented at the *Workshop on Structural Dynamics and Control Interaction of Flexible Structures,* Marshall Space Flight Center, Huntsville, Alabama, April 22-24.

Klepp, H. J., 1990, "Ueber den Einfluss reibungsbehaftcter Bindungen auf den kinetischen Zustand von Mehrkoerpersystem," *Zeitschrift fuer angewandte Mathematik und Physik,* 41, pp. 873-888.

Leonardo da Vinci, 1452-1519, *The Notebooks of Leonardo da Vinci,* translated by Edward MacCurdy, George Braziller, New York (1958).

Liang, J.W., and Feeny, B.F., 1998a, "Dynamical friction behavior in a forced oscillator with a compliant contact," *Journal of Applied Mechanics*, 65(1), pp.250-257.

Liang, J.W., and Feeny, B.F., 1998b, "A comparison between direct and indirect friction measurements in a forced oscillator," Journal of Applied Mechanics, 65(3)m oo, 783-786.

Linker, M. F., and Dieterich, J. H., 1992, "Effects of variable normal stress on rock friction: observations and constitutive equations," *Journal of Geophysical Research* 97, pp. 4923-4940.

Marui, E., and Kato, *S.,* 1984, "Forced vibration of a base-excited single-degree-of-freedom system with Coulomb friction," *Journal of Dynamic Systems, Measurement, and Control* 106, pp. 280-285.

Moon, F. C., 1980, "Experiments on chaotic motions of a forced oscillator: strange attractors," *ASME Journal of Applied Mechanics,* Vol. 47, pp. 638-644.

Moon, F. C., 1992, *Chaotic and Fractal Dynamics,* Wiley-Interscience, New York.

Narayanan, *S.,* and Jayaraman, K., 1991, "Chaotic vibration in a non-linear oscillator with Coulomb friction," *Journal of Sound and Vibration* 146,pp. 17-31.

Nayfeh, A. H., and Mook, D. T., 1979, *Nonlinear Oscillations,* Wiley-Interscience, New York.

Oden, J. T., and Martins, J. A. C., 1985, "Models and Computational Methods for Dynamic Friction Phenomena, *"Computer Methods in Applied Mechanics and Engineering* 52, pp. 527-634.

Polycarpou, A. and Soom, A., 1992, "Transitions between sticking and slipping at lubricated line contacts," *Friction-Induced Vibration, Chatter, Squeal, and Chaos,* ASME Winter Annual Meeting, DE-Vol. 49, pp. 139-148.

Rice, J. R., and Ruina, A. L., 1983, "Stability of steady frictional slipping*," ASME Journal of Applied Mechanics,* Vol. 50, pp. 343- 349.

Rorrer, R., Eiss, N. S., De Togni, R. S., 1992, "Measurement of frictional stick-slip transitions for various elastomeric materials sliding against hard counterfaces," *Wear and Friction of Elastomers,* ASTM Special Technical Publication 1145, pp. 50-64.

Ruina, A. L., 1985, "Constitutive relations for frictional slip," *Mechanics of Geomaterials,* Z. Bazant, ed., John Wiley & Sons Ltd, pp. 169-188.

Ruina, A., 1988, personal communication.

Shaw, S. W., 1986, "On the dynamic response of a system with dry friction," *Journal of Sound and Vibration* 108, pp. 305-325.

Srinivasan, A. V., 1988, "Dynamic friction," *Large Space Structures: Dynamics and Control,* S. N. Atluri and A. K. Amos, eds., Springer-Verlag, New York.

Streator, J. L., 1992, "Considerations of a simplified analysis of transducer dynamics for measuring friction," *ASME Journal of Tribology,* 114, pp. 360-369.

Streator, J. L., and Bogy, D.B., 1992, "Accounting for transducer dynamics in the measurement of friction," *ASME Journal of Tribology,* 114, pp. 86-94.

Tworzydlo, W. W., Becker, E. B., and Oden, J. T., 1992, "Numerical Modeling of friction-induced vibrations and dynamic instabilities," *Friction-Induced Vibration, Chatter, Squeal, and Chaos,* ASME Winter Annual Meeting, DE-Vol. 49, pp. 13-32.

Wojewoda, J., Barron, R., and Kapitaniak, T., 1992, "Chaotic behavior of friction force," *International Journal of Bifurcation and Chaos* 2, pp. 205-209.

Figure Captions

Figure 1. (a) Experimental setup and (b) schematic model for dynamics and friction measurements during oscillations.

Figure 2. An experimental chaotic trajectory from an oscillator with dry friction. The radial axis is x, the circumferential axis is time (modulo the driving period), and the longitudinal axis is $\dot{x}$. The flow is clockwise.

Figure 3. The variation in normal load with displacement for (a) the oscillator with "parallel plates", and (b) the oscillator with skewed plates.

Figure 4. Friction measurements for paper on paper in a regular oscillator driven at 2.5 Hz with amplitude modulation. The normal load ranged from 0.12N to 0.17 N. (a) Coefficient of friction vs. displacement and velocity, (b) the sweep of phase space, (c) Coefficient of friction vs. velocity, (d) coefficient of friction vs. displacement.

Figure 5. Friction measurements for titanium on titanium in a regular oscillator driven at 2.5 Hz with amplitude modulation. The normal load varied from 0.10 N to 0.16 N during oscillation. (a) Coefficient of friction vs. displacement and velocity, (b) the sweep of phase space.

Figure 6. Friction measurement for paper on paper in an oscillator with skewed plates during chaotic motion driven at 4.0 Hz. The normal load varied from 0.04 N to 0.19 N during

oscillation. (a) Coefficient of friction vs. displacement and velocity, (b) the sweep of phase space.

Figure 7. Friction measurement for titanium on titanium in an oscillator with skewed plates during chaotic motion driven at 3.5 Hz. The normal load varied from 0.16 N to 0.47 N during oscillation. (a) Coefficient of friction vs. displacement and velocity, (b) the sweep of phase space.

Figure 8. Friction measurement for paper on paper in a two-well oscillator with parallel plates during chaotic motion driven at 5.0 Hz. The normal load varied from 0.20 N to 0.25 N during oscillation. (a) Coefficient of friction vs. displacement and velocity, (b) the sweep of phase space.

Figure 9. Friction θ verses displacement x and velocity $\dot{x}$ for a simulation of equations (5) and (6) with $a(t) = 2\cos(1.5t)\cos(1.5t/40)$ and $\gamma = 10$.

Figure 10. Numerical simulations of the motivational oscillator using the Coulomb friction law (upper figure), and a state variable friction law (lower figure). Parameter values are a = 1.9, k = 1.5, Ω = 1.25, ζ = 0, and γ = 10. In each figure, x is the radial axis, t(mod $2\pi/\Omega$) is the circumferential axis, and $\dot{x}$ is and the longitudinal axis. The flow is clockwise.

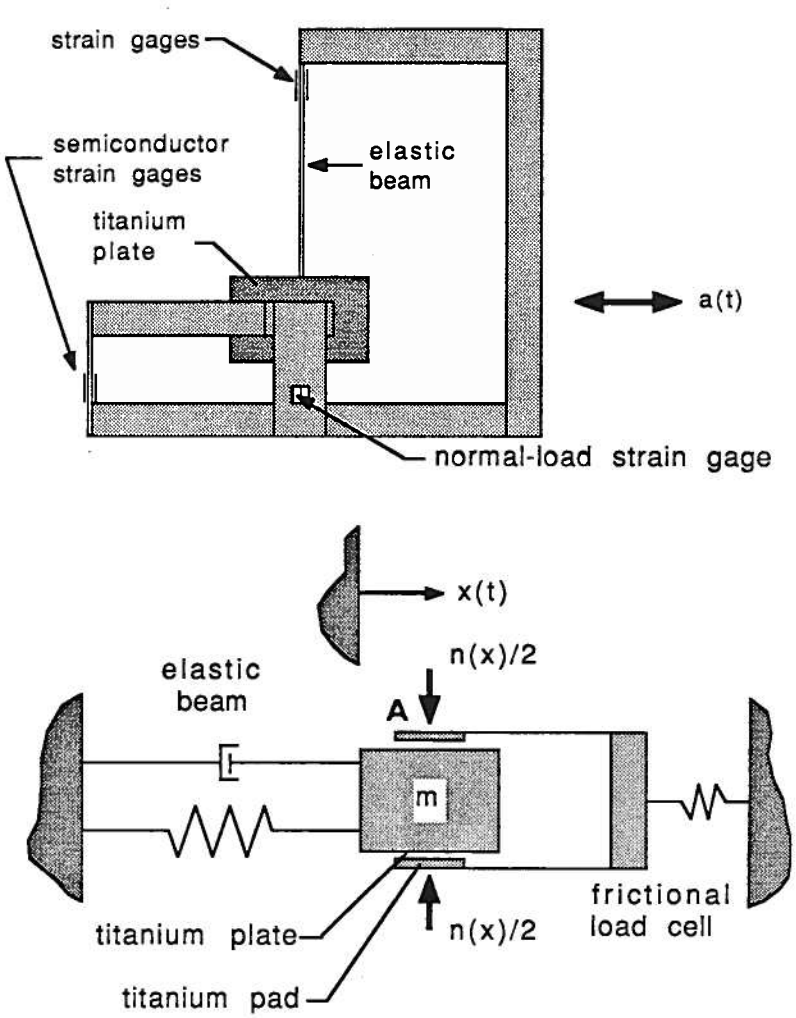

Figure 1. (a) Experimental setup and (b) schematic model for dynamics and friction measurements during oscillations.

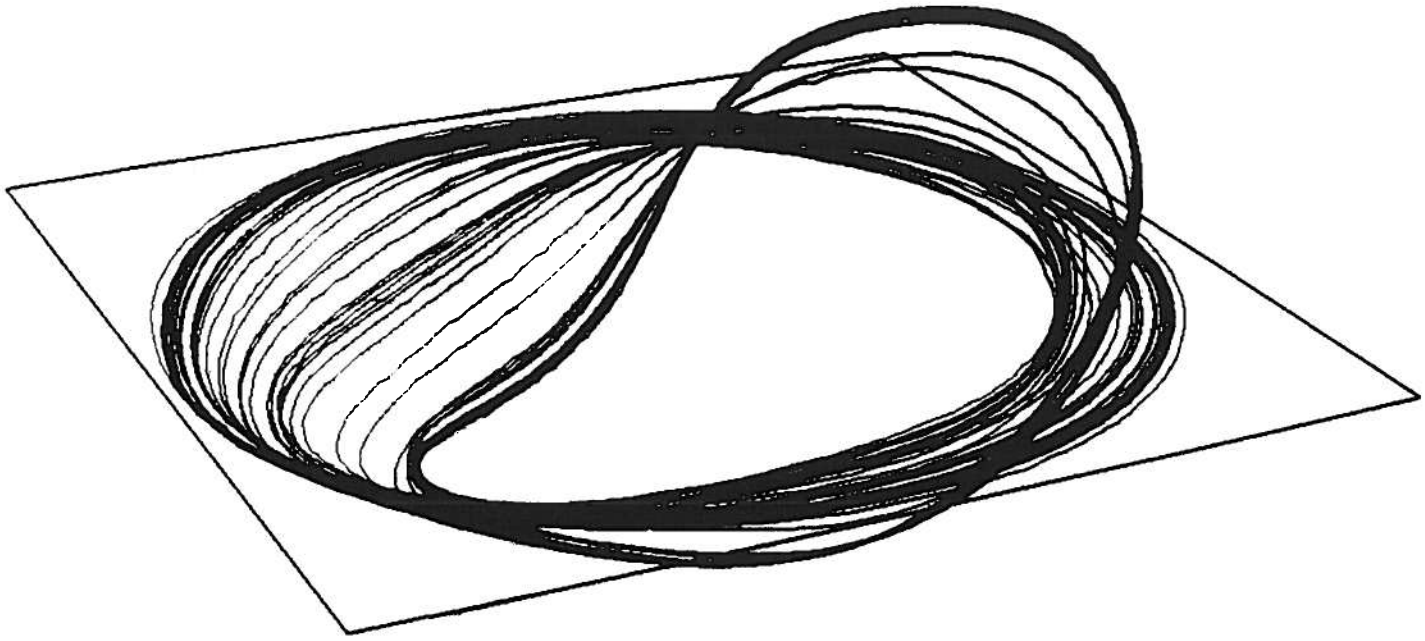

Figure 2. An experimental chaotic trajectory from an oscillator with dry friction. The radial axis is x, the circumferential axis is time (modulo the driving period), and the longitudinal axis is $\dot{x}$. The flow is clockwise.

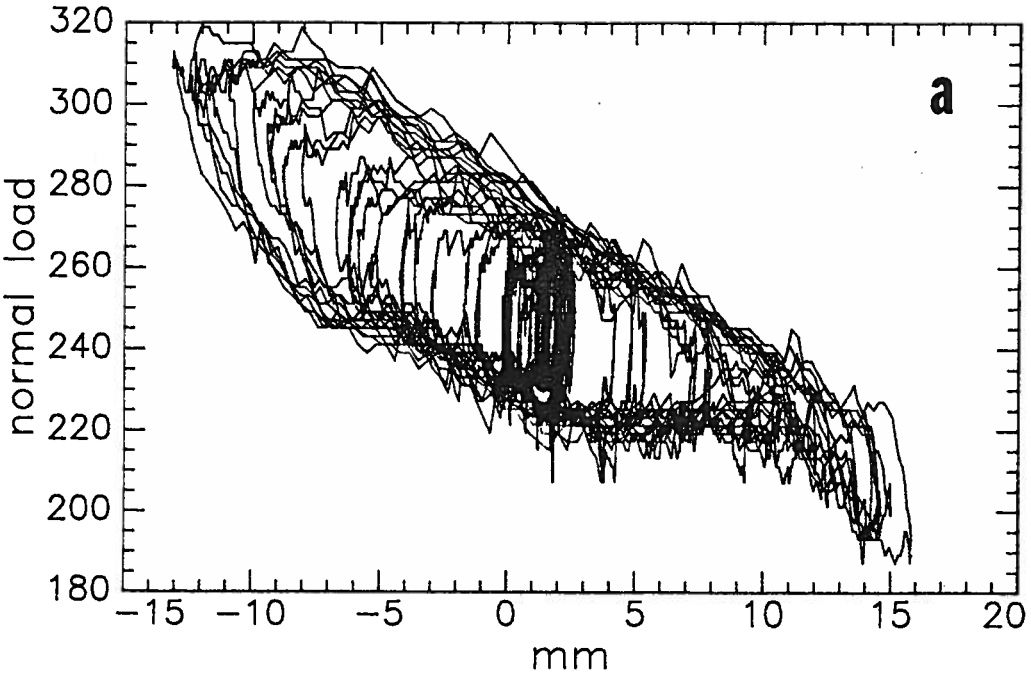
320
300
280
260
240
220
200
180
normal load
−15
−10
−5
0
5
10
15
20
mm
a

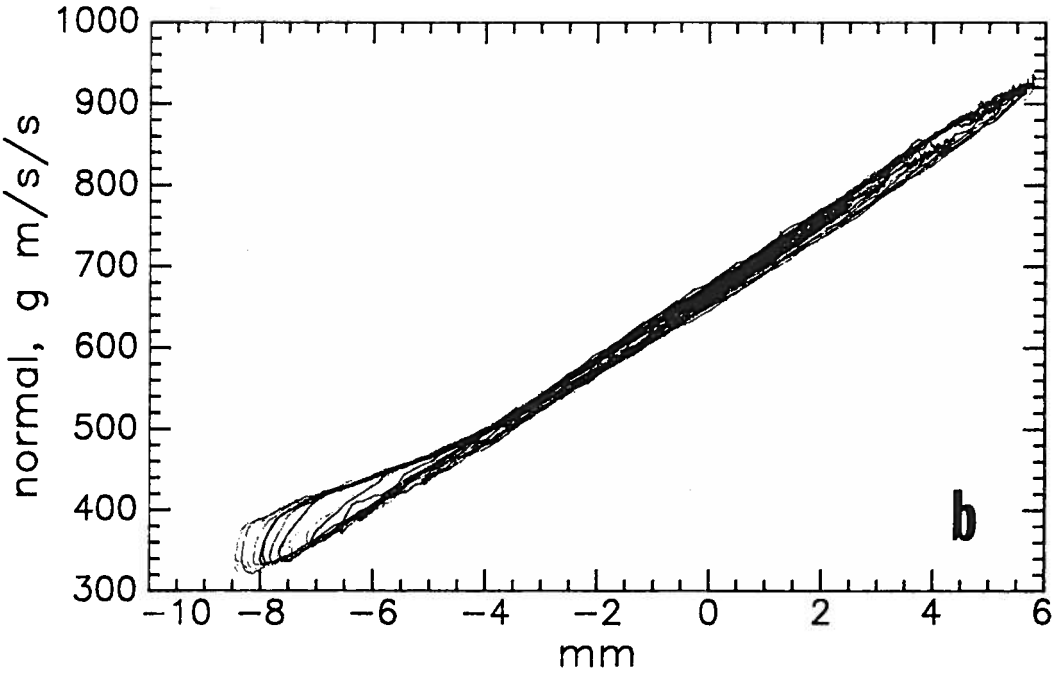

Figure 3. The variation in normal load with displacement for (a) the oscillator with "parallel plates", and (b) the oscillator with skewed plates.

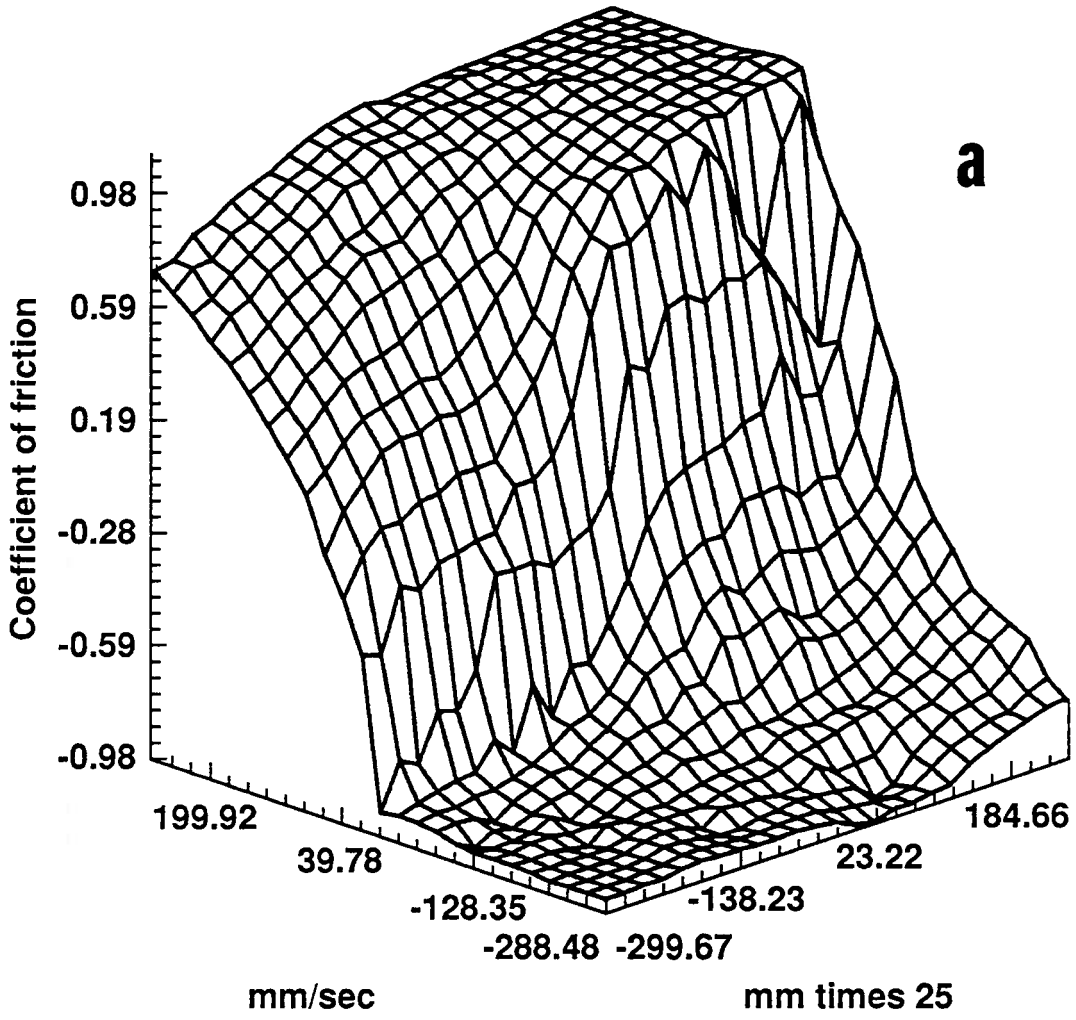

Figure 4. Friction measurements for paper on paper in a regular oscillator driven at 2.5 Hz with amplitude modulation. The normal load ranged from 0.12N to 0.17 N. (a) Coefficient of friction vs. displacement and velocity, (b) the sweep of phase space, (c) Coefficient of friction vs. velocity, (d) coefficient of friction vs. displacement.

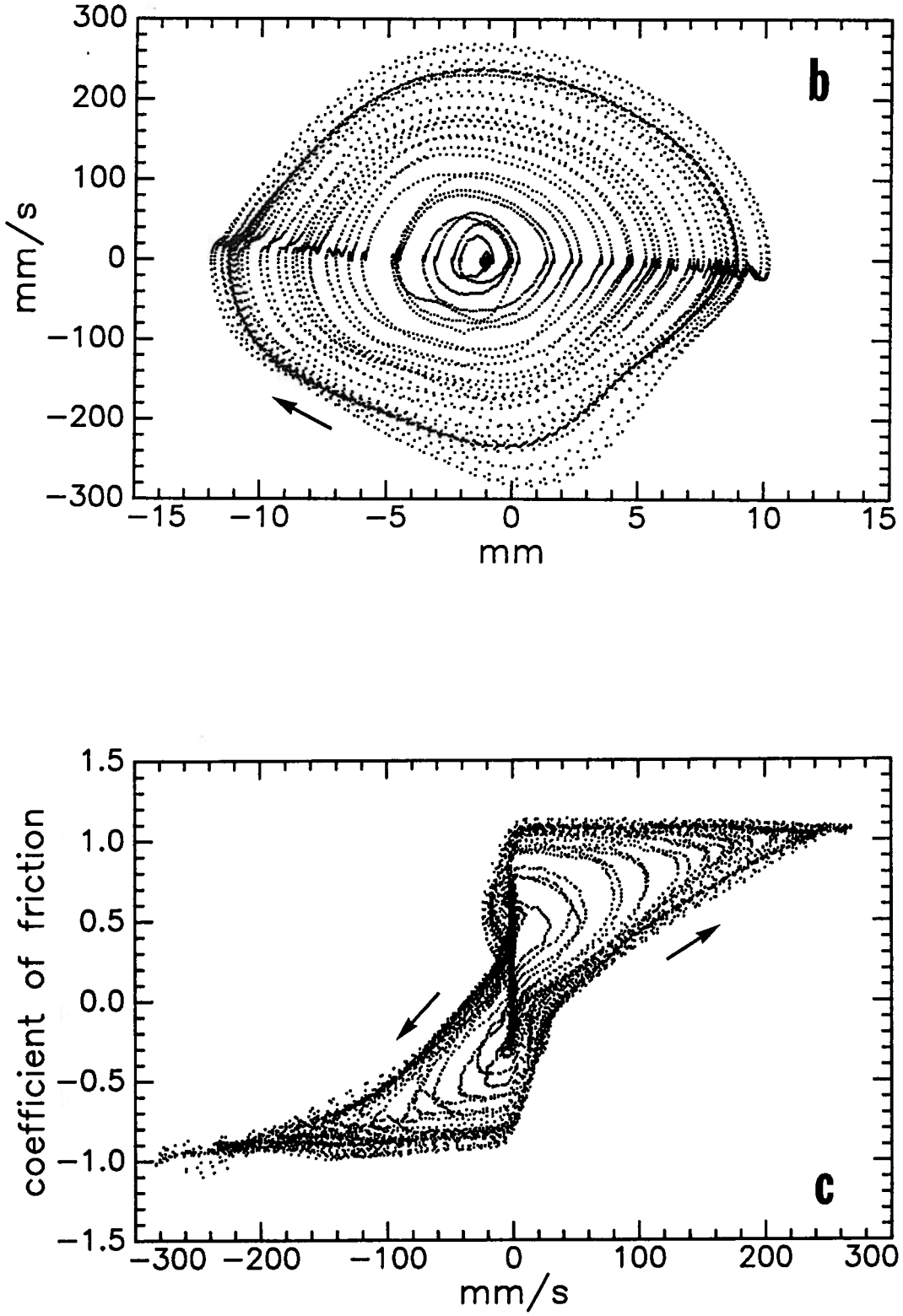

Figure 4. …(b) the sweep of phase space, (c) Coefficient of friction vs. velocity.

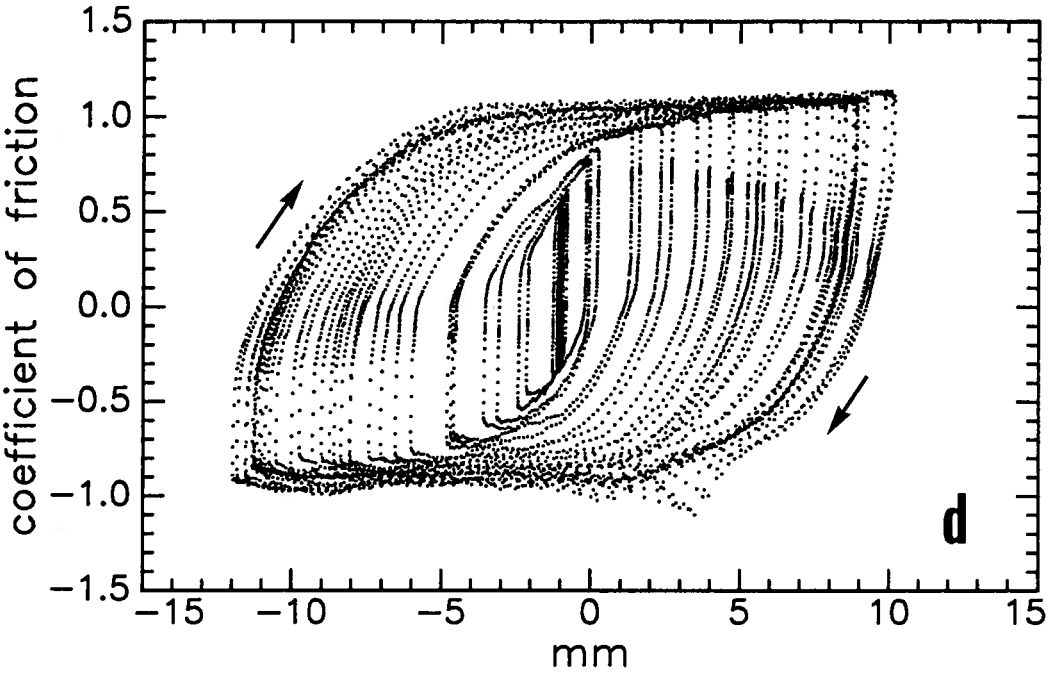

Figure 4. (d) coefficient of friction vs. displacement.

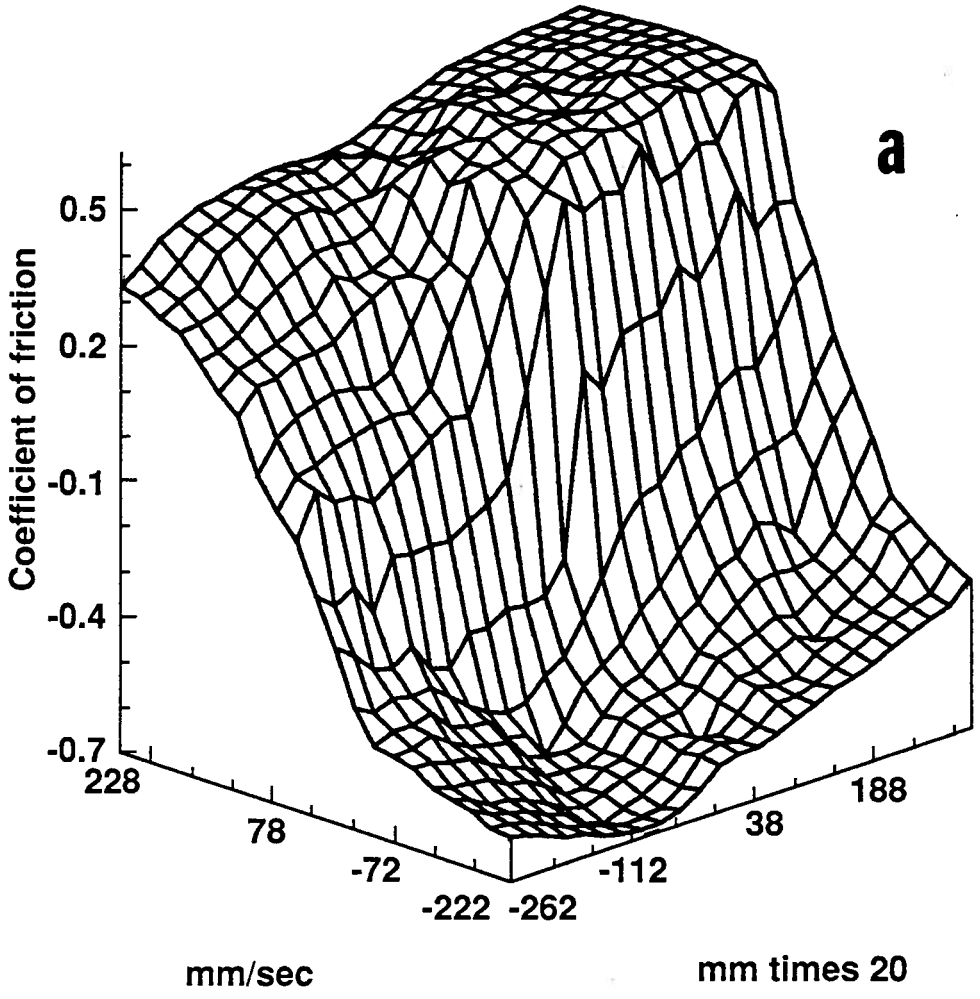

Figure 5. Friction measurements for titanium on titanium in a regular oscillator driven at 2.5 Hz with amplitude modulation. The normal load varied from 0.10 N to 0.16 N during oscillation. (a) Coefficient of friction vs. displacement and velocity, (b) the sweep of phase space.

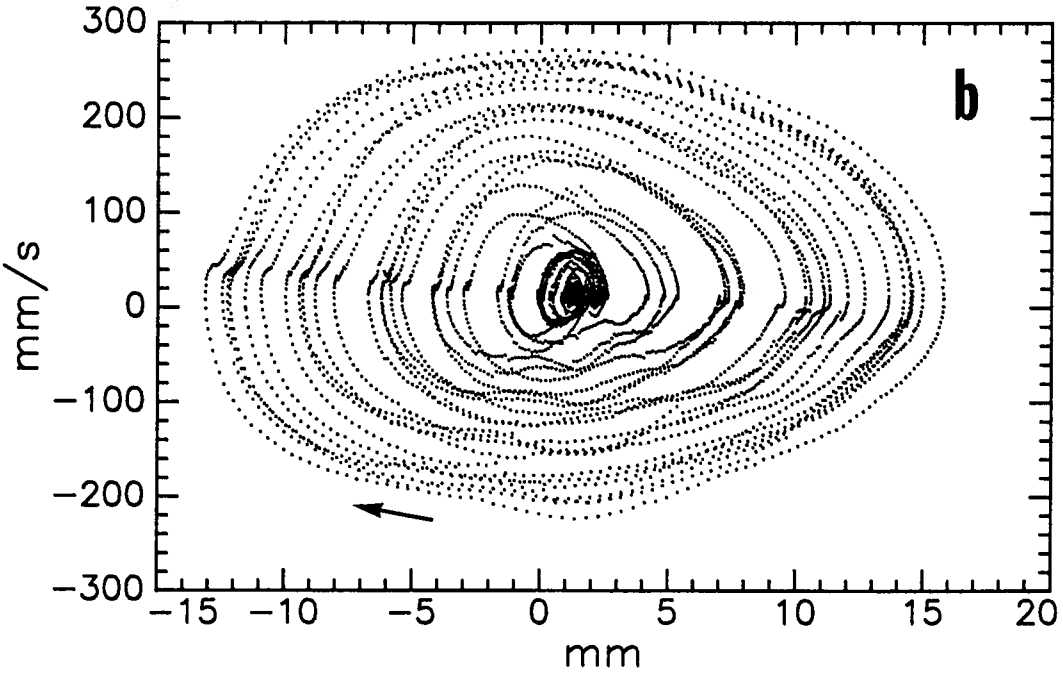

Figure 5. Friction measurements for titanium on titanium in a regular oscillator driven at 2.5 Hz with amplitude modulation. The normal load varied from 0.10 N to 0.16 N during oscillation. (a) Coefficient of friction vs. displacement and velocity, (b) the sweep of phase space.

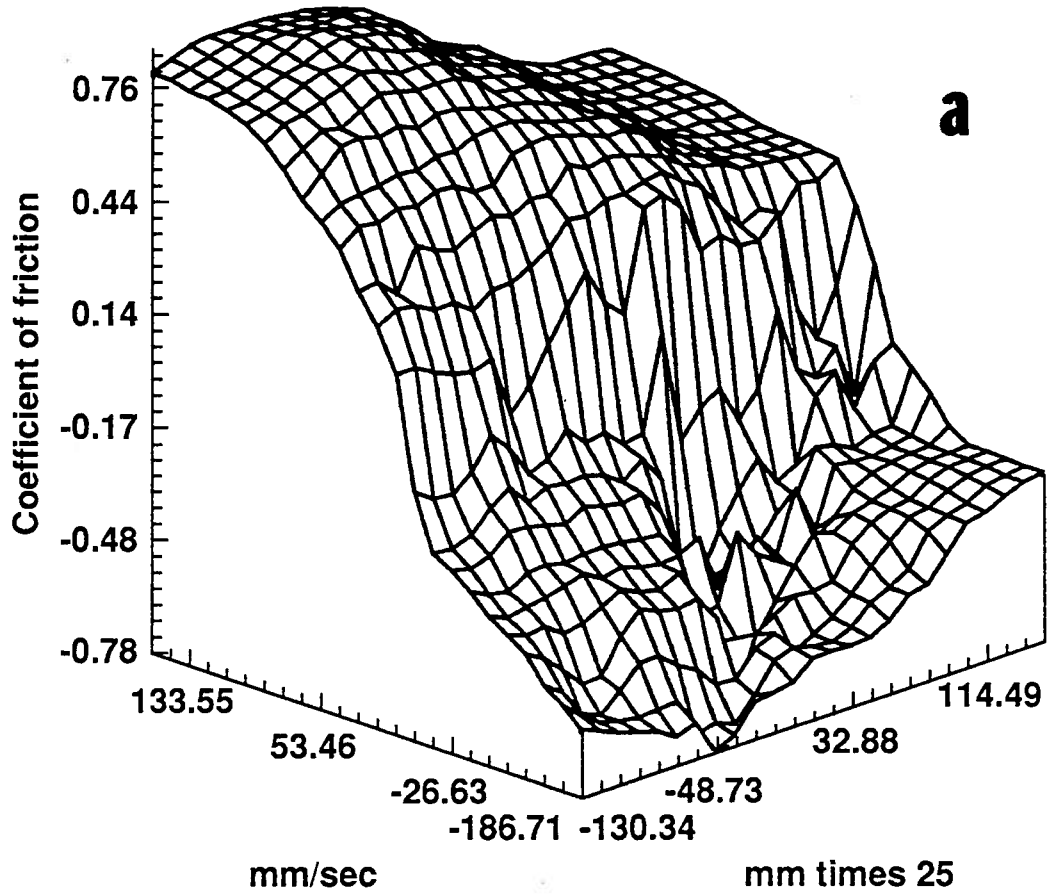

Figure 6. Friction measurement for paper on paper in an oscillator with skewed plates during chaotic motion driven at 4.0 Hz. The normal load varied from 0.04 N to 0.19 N during oscillation. (a) Coefficient of friction vs. displacement and velocity, (b) the sweep of phase space.

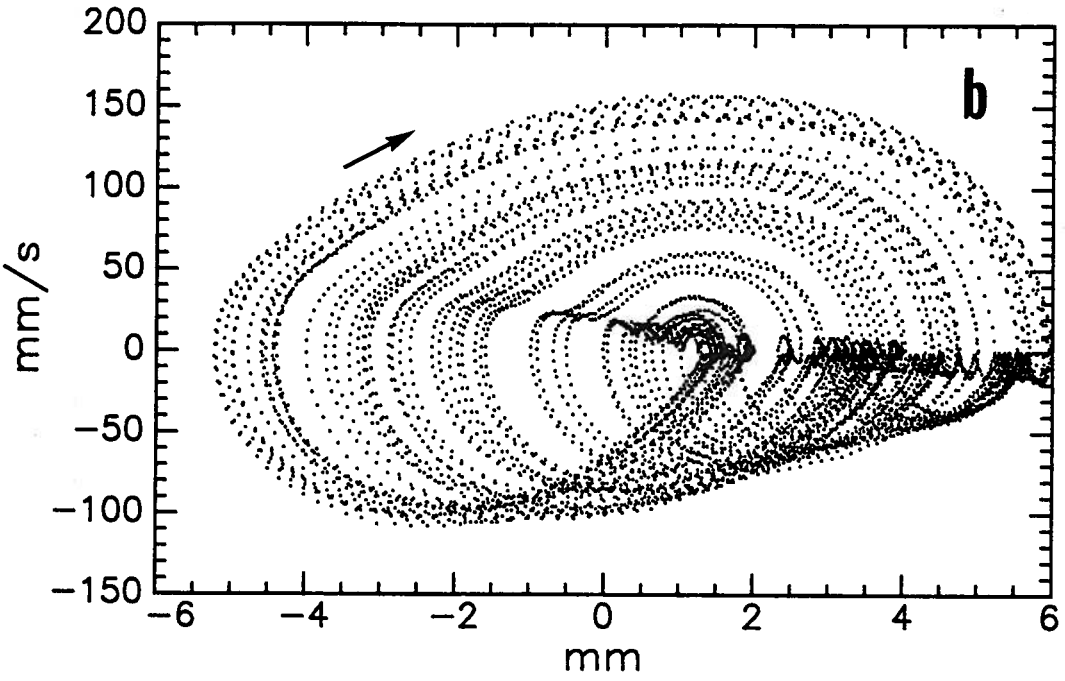

Figure 6. Friction measurement for paper on paper in an oscillator with skewed plates during chaotic motion driven at 4.0 Hz. The normal load varied from 0.04 N to 0.19 N during oscillation. (a) Coefficient of friction vs. displacement and velocity, (b) the sweep of phase space.

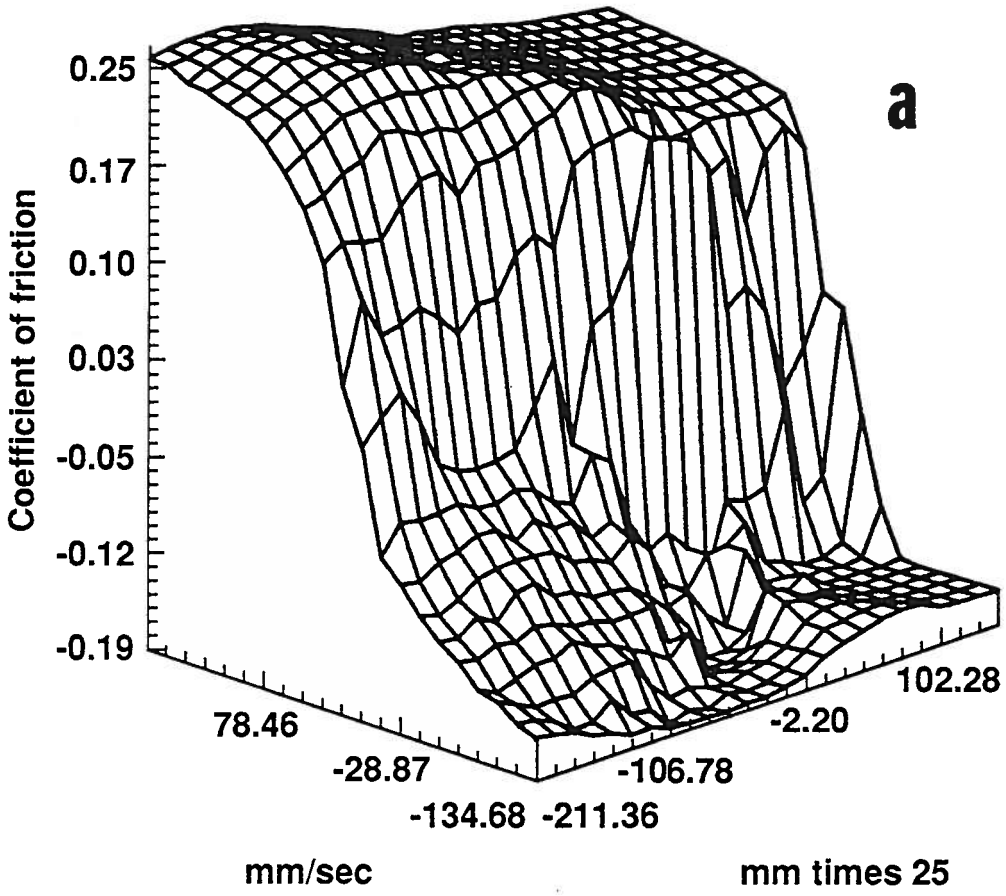

Figure 7. Friction measurement for titanium on titanium in an oscillator with skewed plates during chaotic motion driven at 3.5 Hz. The normal load varied from 0.16 N to 0.47 N during oscillation. (a) Coefficient of friction vs. displacement and velocity, (b) the sweep of phase space.

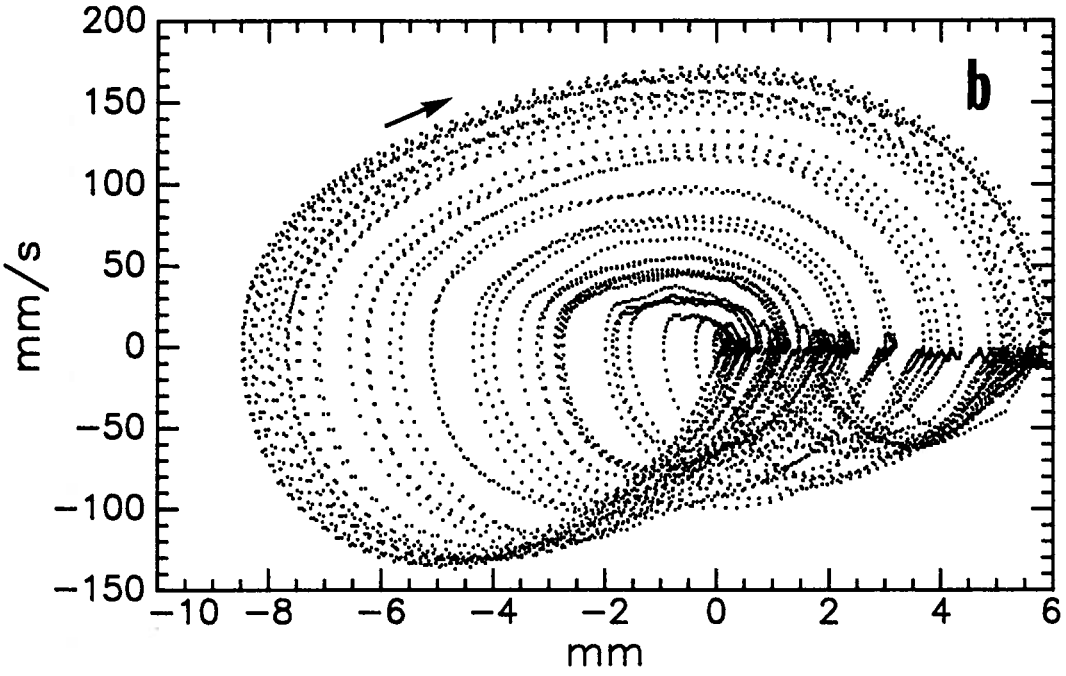

Figure 7. Friction measurement for titanium on titanium in an oscillator with skewed plates during chaotic motion driven at 3.5 Hz. The normal load varied from 0.16 N to 0.47 N during oscillation. (a) Coefficient of friction vs. displacement and velocity, (b) the sweep of phase space.

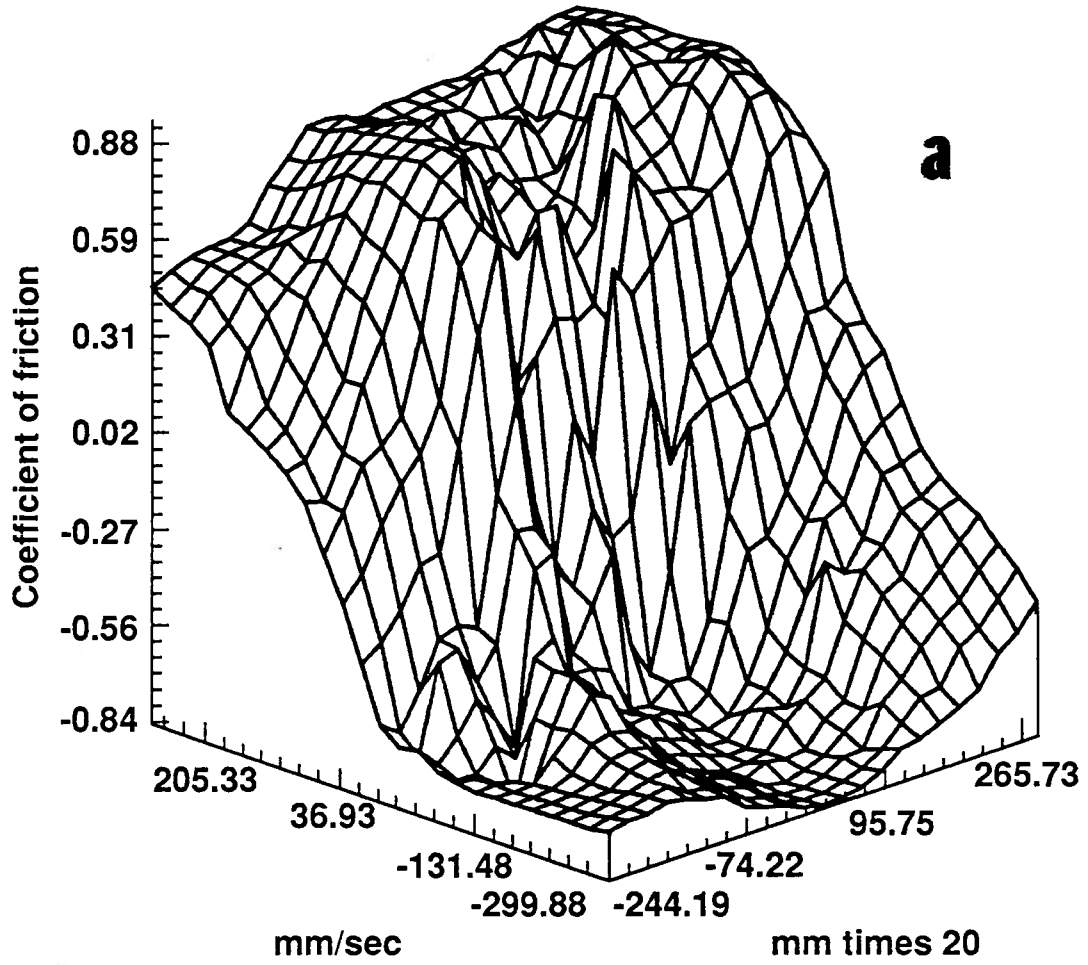

Figure 8. Friction measurement for paper on paper in a two-well oscillator with parallel plates during chaotic motion driven at 5.0 Hz. The normal load varied from 0.20 N to 0.25 N during oscillation. (a) Coefficient of friction vs. displacement and velocity, (b) the sweep of phase space.

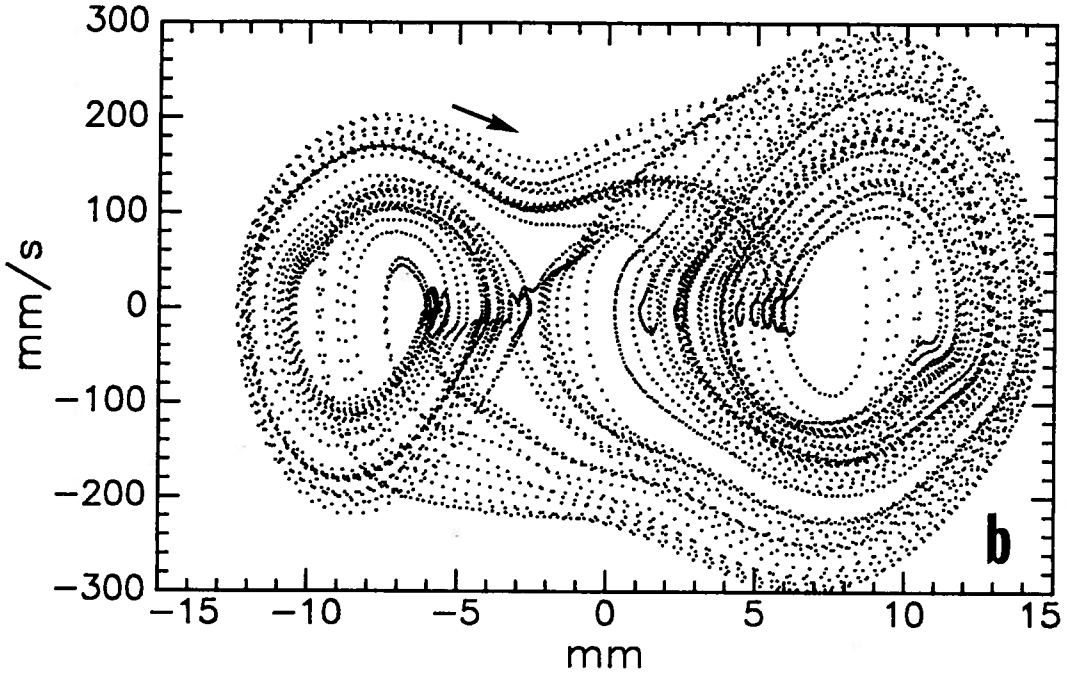

Figure 8. Friction measurement for paper on paper in a two-well oscillator with parallel plates during chaotic motion driven at 5.0 Hz. The normal load varied from 0.20 N to 0.25 N during oscillation. (a) Coefficient of friction vs. displacement and velocity, (b) the sweep of phase space.

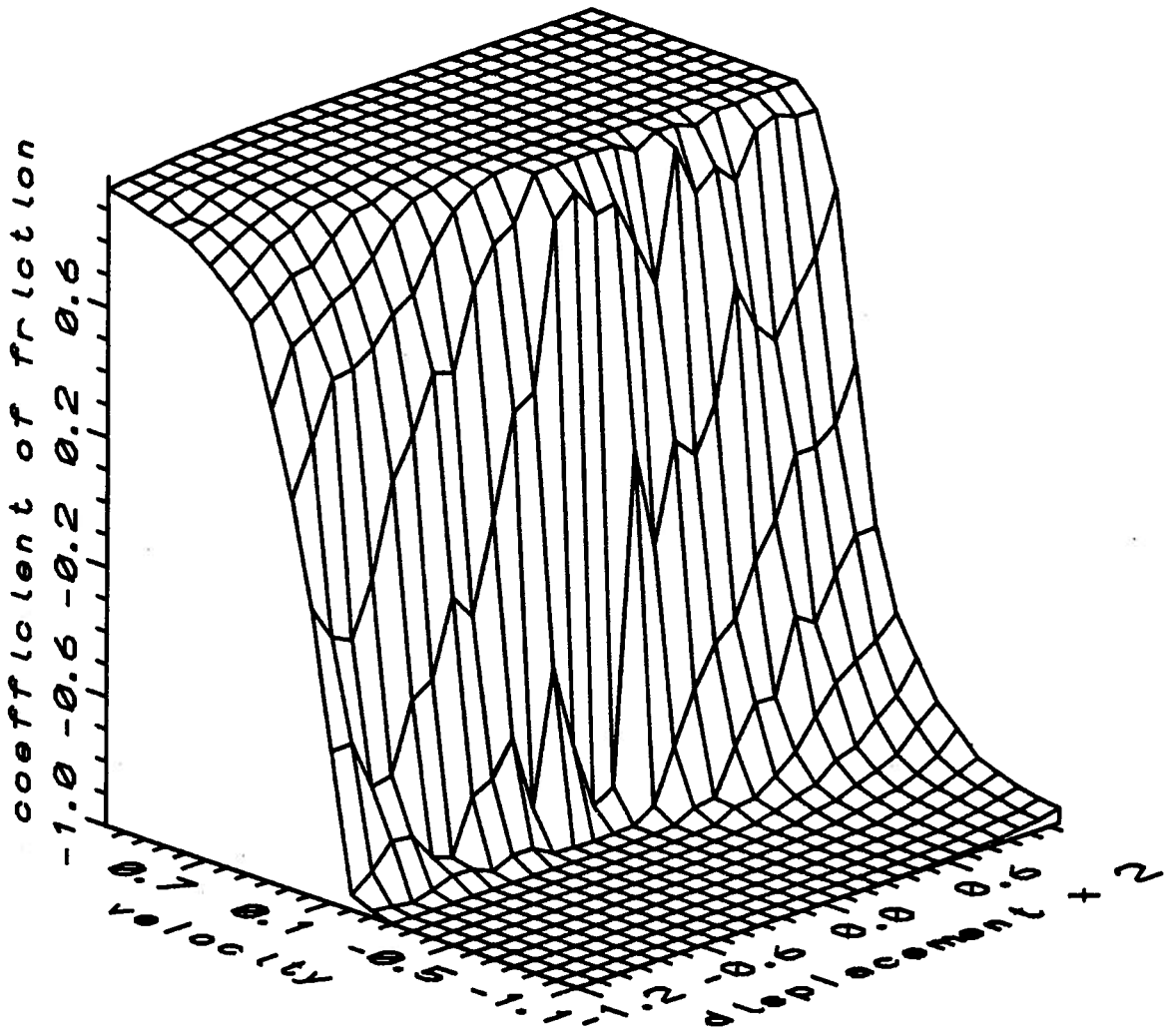

Figure 9. Friction θ verses displacement x and velocity $\dot{x}$ for a simulation of equations (5) and (6) with $a(t) = 2\cos(1.5t)\cos(1.5t/40)$ and $\gamma = 10$.

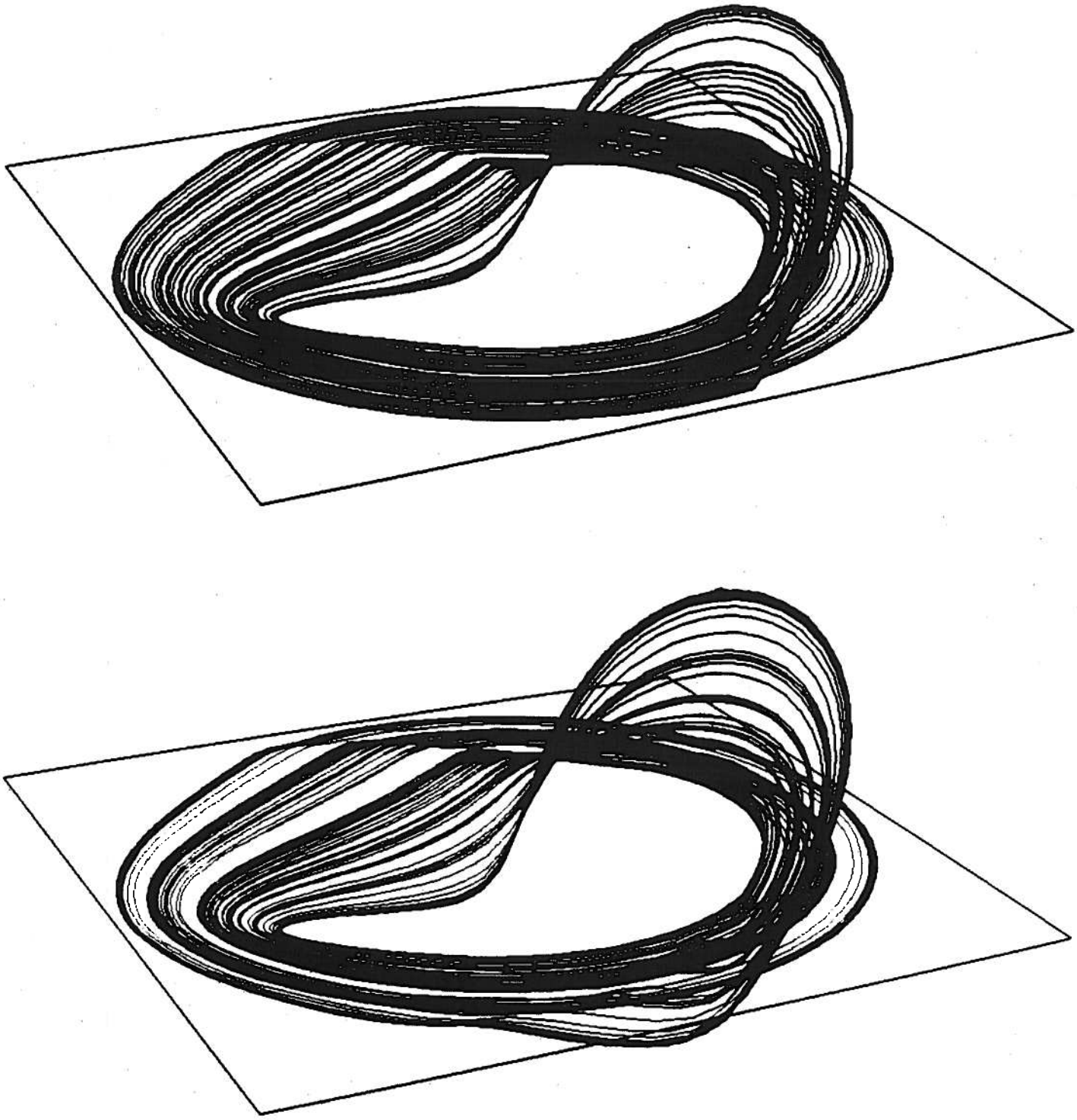

Figure 10. Numerical simulations of the motivational oscillator using the Coulomb friction law (upper figure), and a state variable friction law (lower figure). Parameter values are a = 1.9, k = 1.5, Ω = 1.25, ζ = 0, and γ = 10. In each figure, x is the radial axis, t(mod $2\pi/\Omega$) is the circumferential axis, and $\dot{x}$ is and the longitudinal axis. The flow is clockwise.